

# A SURVEY OF THE SOUTHERN SKY AT 85 MHz

By K. W. YATES,\* R. WIELEBINSKI,\* and T. L. LANDECKER\*

[*Manuscript received June 1, 1967*]

## *Summary*

A survey at 85 MHz is presented of the sky south of declination  $\delta = -20^\circ$ , and of the northern galactic spur region to  $\delta = +20^\circ$ . The survey was made with the 210 ft telescope at Parkes, New South Wales. At this frequency the observed beamwidth was  $3.5^\circ$  by  $3.8^\circ$  to half-power points. The radiation characteristics of the survey aerial and of scaled aerial models were studied to enable corrections to be made for radiation received by the aerial from regions outside the main beam. Absolute beam temperatures derived from the observed aerial temperatures had an r.m.s. accuracy of better than 7%.

## I. INTRODUCTION

A number of accurate sky surveys have been made of the background radio emission at metre wavelengths in the northern hemisphere. Less information is available about the southern sky. For this reason the accurate survey described in the present paper has been made at 85 MHz with an aerial of medium resolution.

A survey of the northern sky at 81.5 MHz was made by Baldwin (1955*a*) with an aerial beam  $2^\circ$  by  $15^\circ$ . On the basis of this survey a model of the galactic radio emission was set up. This model consisted of a disk of emitting regions close to the galactic plane and a surrounding halo (Baldwin 1955*b*). Surveys by Turtle and Baldwin (1962) at 178 MHz and by Pauliny-Toth and Shakeshaft (1962) at 404 MHz contributed further to the understanding of the galactic emission. In these surveys of the northern sky, accurate aerial temperature measurements, calibrated essentially in terms of absolute thermal standards, were made. The measured aerial temperatures were reduced to beam temperatures from experimentally derived aerial radiation characteristics.

In the southern hemisphere Mills, Hill, and Slee (1958) made a survey at 85 MHz with a resolution of  $50'$ , concentrating on the features near the galactic plane. Averaged observations away from the galactic plane were presented by Mills (1959) in the form of a galactic map. The nature of the aerial used in these observations precluded absolute calibrations. The present survey, which was made with a paraboloidal reflector, is accurately calibrated, giving, for the first time, southern sky maps comparable with those available for the northern sky.

\* School of Electrical Engineering, University of Sydney.

The need for accuracy is demonstrated by the doubts raised by Baldwin (1963) about the validity of the galactic disk and halo model. Furthermore, for lack of accurate southern sky surveys the many spurs of emission observed in the north could not be followed around the sky.

The CSIRO 210 ft diameter paraboloidal reflector at Parkes was used for the present survey. Beamwidths in the cardinal planes using a dipole-reflector feed were measured as  $3\cdot5^\circ$  and  $3\cdot8^\circ$ , from scans of strong radio sources. Particular care was taken to make accurate absolute measurements of aerial temperature. To derive accurate beam temperatures from these measurements, the radiation characteristics of the survey aerial itself, and of scaled models of it, were investigated. While it would have been preferable to carry out these experiments entirely with the survey aerial, we were compelled to resort to the use of models by the restricted availability of the Parkes telescope. The derivation of beam temperatures from aerial temperatures is most important, since it is the beam temperature that describes actual sky brightness. In the present survey this question has been investigated in sufficient detail to justify a claimed r.m.s. accuracy of 7% for the beam temperatures presented.

The survey covers the southern sky below the declination  $\delta = -20^\circ$ . Additional observations were made of the northern galactic spur feature up to  $\delta = +20^\circ$ .

## II. APPARATUS

The aerial used for this survey was the 210 ft fully steerable paraboloidal reflector at Parkes, New South Wales. At 85 MHz the aperture is some  $18\lambda$  in diameter ( $\lambda = 3\cdot5$  m). The primary feed was a  $\frac{1}{2}\lambda$  dipole mounted at the focus  $0\cdot1\lambda$  below the reflecting area of the aerial cabin, which is one wavelength in diameter at our frequency. The tripod structure supporting the feed was close to the primary feed and its interaction could not be disregarded. The reflector is altitude–azimuth mounted and it was possible to place the dipole so that the  $E$  plane was always vertical. One tripod leg lay in this plane. The dipole feed was matched to an impedance of  $50\ \Omega$  by adjustment of dipole dimensions and of distance from the reflecting plate.

The receiver is shown as a block diagram in Figure 1. It was a switched radio-meter in which the receiver output was linearly dependent on the difference at the two inputs of the synchronously driven switch SW2. One input of the switch was connected to a reference load held at ambient temperature. The second input to the switch could be connected either to the aerial or to a noise source depending on the position of the switch SW1. This second switch was remotely controlled and allowed monitoring of zero level and calibration from a noise generator. The losses in the two switches were measured and found to be  $0\cdot1$  dB with isolation of  $> 30$  dB.

The solid state preamplifier and mixer were mounted in the aerial cabin at the focus a few feet from the dipole. The intermediate frequency output at 30 MHz with a bandwidth of 800 kHz was connected to the control room by a low loss coaxial cable. The following receiver stages were housed in the control room near the pen recorder. Receiver detector output was monitored through an audio amplifier during the observing period to reveal interference.

The noise source used for calibration was a diode noise source described by Harris (1961). This noise source presents a good matched load in the cold condition, allowing zero-level check. Harris claimed an absolute accuracy of 1% for the noise output as a function of diode current. This accuracy was verified by us in calibrations of the noise source against thermal loads at 77, 293, and 373°K.

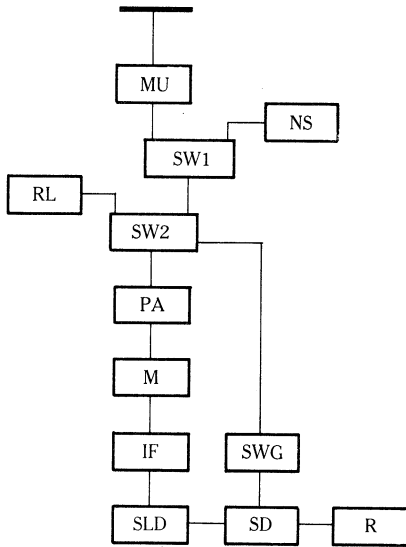


Fig. 1.—Receiver block diagram:

MU	matching unit
SW1	switch
SW2	switch
NS	noise source
RL	reference load
PA	85 MHz preamplifier
M	mixer
IF	30 MHz i.f. amplifier
SLD	square-law detector
SD	synchronous detector
SWG	switching waveform generator
R	pen recorder

### III. OBSERVATIONAL METHODS

The receiver output was proportional to the difference in noise power available at the two inputs to the synchronous switch, i.e. to

$$T_e - T'_r,$$

where  $T_e$  is the aerial temperature and  $T'_r$  the reference load temperature as modified by lossy components. The effective aerial temperature  $T_e$  is related to the loss-free aerial temperature  $T_i$  by

$$T_e = (1-\alpha)T_i + \alpha T_a,$$

where  $\alpha$  is the loss factor and  $T_a$  the temperature of the lossy components. A similar expression relates  $T'_r$  to the actual temperature  $T_r$  of the reference load. Receiver output was proportional to

$$\{T_i(1-\alpha) + \alpha T_a - T_r(1-\alpha') - \alpha' T_a\},$$

where  $\alpha'$  is the loss factor on the reference load side.

The proportions of the available power from the aerial and calibrating source that were transferred to the receiver would have been the same only when each had

the same impedance function across the entire receiver bandwidth. After initial adjustment of the dipole, the aerial impedance was maintained at  $50 \Omega$  by periodic adjustment of the double stub matching unit (MU in Fig. 1). Adjustments were made at the centre frequency; measurements, using a GR admittance meter type 1602-B, indicated a standing wave ratio (s.w.r.) of 1.05 over the complete pass band, deteriorating to 1.1 just outside the band. This compared with a frequency-independent s.w.r. of 1.02 for the calibrating source. Over much of the sky the aerial temperatures were so high that a 6 dB attenuator could be used between aerial and receiver, minimizing effects of impedance mismatch.

The observations were made on four nights in July 1966. Most of the observations consisted of declination scans in sweeps of  $20^\circ$  at a driving rate of  $2\frac{1}{2}$  deg/min. At the end of each scan, zero level was checked and a noise calibration recorded. The south celestial pole and strong radio sources were observed from time to time as a system performance check. In the high temperature regions overlapping scans were made. In the colder sky regions adjoining scans were made. After scanning was complete the temperatures of a grid of points across the sky were accurately measured to ensure the consistency of the survey.

#### IV. AERIAL PARAMETERS AND THE REDUCTION OF SURVEY MEASUREMENTS

To derive beam temperatures from aerial temperatures the radiation characteristics of the survey aerial must be known. The reduction method used follows a similar reduction presented by Seeger *et al.* (1964).

A loss-free aerial with normalized response pattern  $f(\theta, \phi)$  placed in a temperature environment  $T(\theta, \phi)$  assumes an aerial temperature  $T_i$  given by

$$T_i = \Omega^{-1} \int_{4\pi} T(\theta, \phi) f(\theta, \phi) d\omega,$$

where  $(\theta, \phi)$  are spherical coordinates of a unit sphere,  $d\omega$  is an element of solid angle, and  $\Omega$  is the aerial solid angle defined by

$$\Omega = \int_{4\pi} f(\theta, \phi) d\omega.$$

Aerial solid angle  $\Omega$  is related to aerial directivity  $D$  by

$$\Omega = 4\pi/D.$$

For large reflecting aerials it is convenient to divide the response pattern into three sections that contribute separately to the aerial noise power. They are the regions B, S, and G; region B comprises the main forward response of the aerial; S is the region of the aerial's forward sidelobes; G is the region where the ground radiates into the feed spillover response. Then

$$\Omega = \Omega_B + \Omega_S + \Omega_G.$$

$\Omega_B$  is the full-beam solid angle. We arbitrarily set its limits  $8^\circ$  from the axis, to include the main beam and the first sidelobes. The region G is between  $90^\circ$  and  $115^\circ$  from the axis. The remaining directions, filled with the minor sidelobes of the aerial, comprise S.

Noise contributions from these three regions add at the aerial terminals, and the loss-free aerial temperature  $T_i$  is related to the mean temperature  $T_B$ ,  $T_S$ , and  $T_G$  in each region by

$$T_i = (\Omega_B/\Omega)T_B + (\Omega_S/\Omega)T_S + (\Omega_G/\Omega)T_G.$$

Derivation of  $T_B$ , the full-beam temperature, from the knowledge of aerial temperature  $T_i$  requires knowledge of the aerial parameters and mean temperatures in the sidelobe and ground regions.

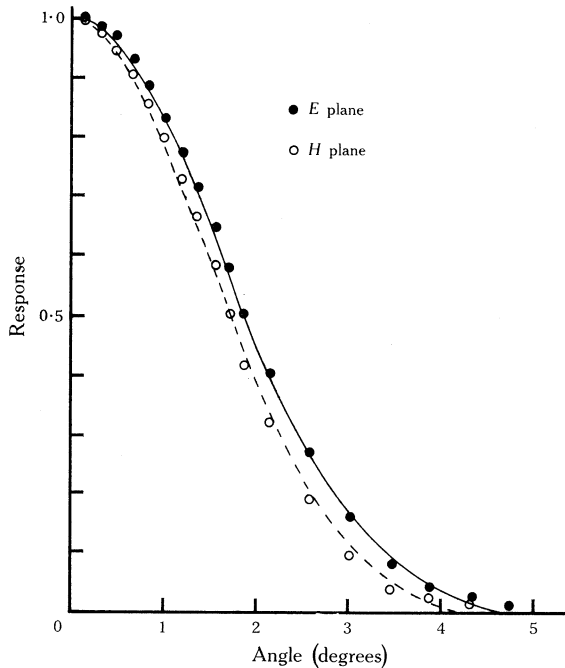


Fig. 2.—Observed polar patterns of the aerial compared with Gaussian response curves.

During the observations a full picture of the main beam was built up from scans through the sources Fornax, Pictor, Virgo, and Hydra at various parallactic angles. The  $E$  and  $H$  patterns derived from these observations are shown in Figure 2, each compared with a Gaussian response. The radio sources were too weak to reveal any sidelobes accurately. The first sidelobes were estimated from pattern measurements of a scaled reflector. One of the 45 ft diameter reflectors (Christiansen and Wellington 1966) at the Fleurs Field Station of the School of Electrical Engineering was used at the frequency of 408 MHz with the Sun as source. At this frequency the 45' reflector scales almost exactly the Parkes reflector at 85 MHz. The only item not scaled exactly was the feed. An axial tube was used at Fleurs instead of the tripod structure used at Parkes. For this reason only the main beam and first sidelobes observed at Fleurs could be taken to represent the survey aerial diagrams. The composite polar pattern deduced from these measurements is shown in Figure 3.

This composite pattern was integrated out to  $8^\circ$  yielding

$$\Omega_B = 4.5 \times 10^{-3} \quad \text{steradian}^2.$$

For a Gaussian response

$$\Omega_B = 1.133 \theta_E \theta_H,$$

where  $\theta_E$  and  $\theta_H$  are the  $E$  and  $H$  plane half-power beamwidths (Seeger *et al.* 1964). Our measured values of  $3.8^\circ$  and  $3.5^\circ$  also gave

$$\Omega_B = 4.5 \times 10^{-3} \quad \text{steradian}^2.$$

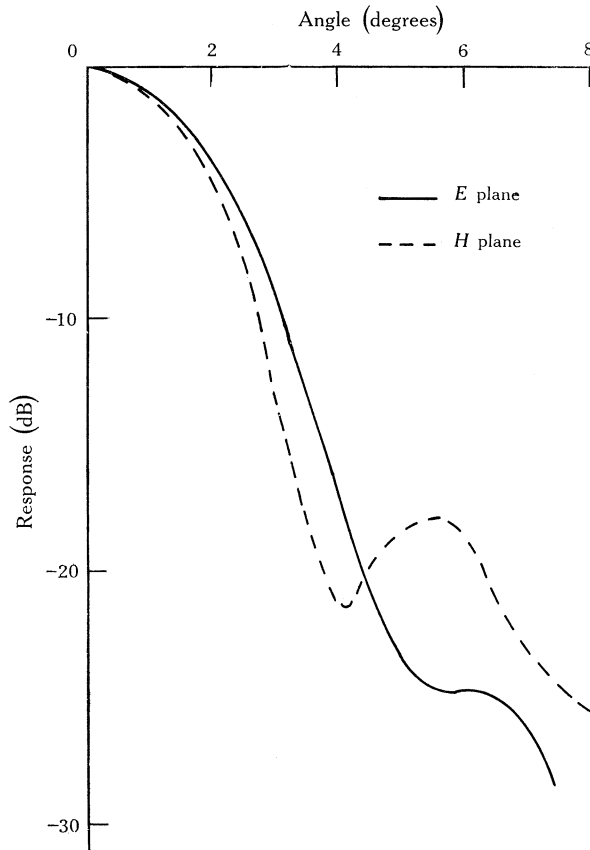


Fig. 3.—Composite polar pattern derived from observations and scaled aerial measurements.

The quantity  $\Omega_G/\Omega$  was found by the integration of the radiation patterns of models of the primary feed and tripod structure. Two models were built and tested in the Aerials Laboratory of the School of Electrical Engineering. A model at 3 cm wavelength scaled well the tripod and the edge of the reflector but could not accurately represent the dipole-balun arrangement. A second model at 10 cm wavelength scaled the dipole and the balun but could not scale the total length of the tripod

legs. Experiments over a dynamic range of 40 dB with these models gave radiation patterns in the cardinal planes. A composite radiation pattern was obtained, which was taken to represent the primary polar pattern of the survey aerial. If the feed pattern is  $g(\theta, \phi)$ , by integration we obtained

$$\left\{ \int_{90^\circ}^{115^\circ} g(\theta, \phi) d\omega \right\} \left\{ \int_{4\pi} g(\theta, \phi) d\omega \right\}^{-1} = 0.19.$$

The secondary response of the reflector in the spillover region is essentially that of the feed, and therefore

$$\Omega_G/\Omega = 0.19.$$

The most difficult aerial parameter to measure is the solid angle  $\Omega_S$  corresponding to the sidelobe regions. It is the smallest numerically, and therefore an estimate should be sufficiently accurate. From published measurements of the radiation patterns of paraboloidal reflectors and from direct measurements using the 45 ft reflector at Fleurs we concluded that the response could be taken as 35 dB down for one half of the solid angle and 50 dB down for the other half. From this assumption

$$\Omega_S = 9.5 \times 10^{-4} \quad \text{steradian}^2.$$

From these results we can deduce

$$\Omega_B = 4.5 \times 10^{-3} \quad \text{steradian}^2,$$

$$\Omega_S = 0.95 \times 10^{-3} \quad \text{steradian}^2,$$

$$\Omega_G = 1.3 \times 10^{-3} \quad \text{steradian}^2,$$

$$\Omega = 6.75 \times 10^{-3} \quad \text{steradian}^2.$$

These values can be checked in two ways. The directivity of the aerial  $D$  is

$$D = 4\pi/\Omega$$

and its aperture efficiency  $\eta_a$  is

$$\eta_a = (4\pi/\Omega)(\lambda^2/4\pi A),$$

where  $A$  is the area of the aperture. Thus the aperture efficiency is

$$\eta_a = 58\%,$$

which is in good agreement with published values of about 55% for the same reflector at higher frequencies (Minnett and Yabsley 1966).

Aerial temperatures were measured from scans of sources Fornax, Pictor, Virgo, and Hydra. Flux values for these sources are available from the catalogues of Mills, Slee, and Hill (1960, 1961) and Conway, Kellerman, and Long (1963). A point source of flux density  $S$  produces an aerial temperature  $T_i$  given by

$$T_i = S\lambda^2/2k\Omega,$$

where  $k$  is the Boltzmann constant. Our source measurements are grouped in Table 1. From the four measurements we obtain the mean value of the ratio  $S/T_i$  as

$$S/T_i = 1.6,$$

which leads to

$$\Omega = 7 \times 10^{-3} \quad \text{steradian}^2.$$



Figs. 4(a)–4(c).—Sky maps of modified beam temperatures drawn in equatorial coordinates. Note that in (b) the maximum observed temperature at  $l = 0, b = 0$  is  $16\,000^\circ\text{K}$ .

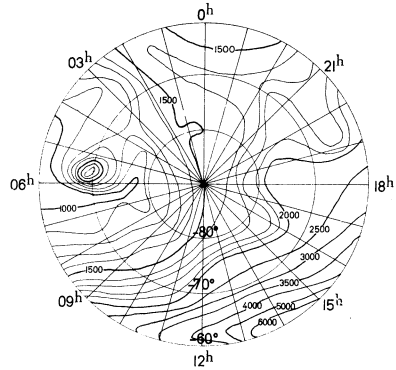


Fig. 4(c)

Having found the aerial solid angles for the full-beam, sidelobe, and ground regions, we could then derive the full-beam temperatures  $T_B$  from the equation

$$T_B = (\Omega/\Omega_B)T_i - (\Omega_S/\Omega_B)T_S - (\Omega_G/\Omega_B)T_G.$$

Even with the knowledge of the aerial parameters, the derivation of full-beam temperatures involves formidable computational difficulties.  $T_S$  and  $T_G$  must be estimated for all directions.  $T_G$  changed with aerial elevation, since away from the zenith the spillover region intercepted partly ground and partly sky. Therefore we

TABLE 1  
SOURCE MEASUREMENTS

Source	$S$ (flux units)	Catalogue Reference	Observed Temperature $T_i$ ( $^\circ\text{K}$ )	$S/T_i$
Fornax	950	Mills 03–31	630	1.5
Pictor	570	Mills 05–43	440	1.3
Virgo	1900	Conway 3C274	1090	1.7
Hydra	690	Mills 09–14	379	1.8

decided to reduce our results more simply, deriving “modified beam temperatures”, and to make complete derivations of full-beam temperatures for only a few directions to enable us to estimate the error introduced by our simplifications.

The full-beam temperature  $T_B$  is the closest approximation to the true brightness distribution  $T(\theta, \phi)$  that the aerial will allow us to derive,

$$T_B = \Omega_B^{-1} \int_{\Omega_B} T(\theta, \phi) f(\theta, \phi) d\omega.$$

The full-beam temperature  $T_B$  is the mean of the temperature distribution weighted by the aerial response over the full beam. We present our results as the weighted

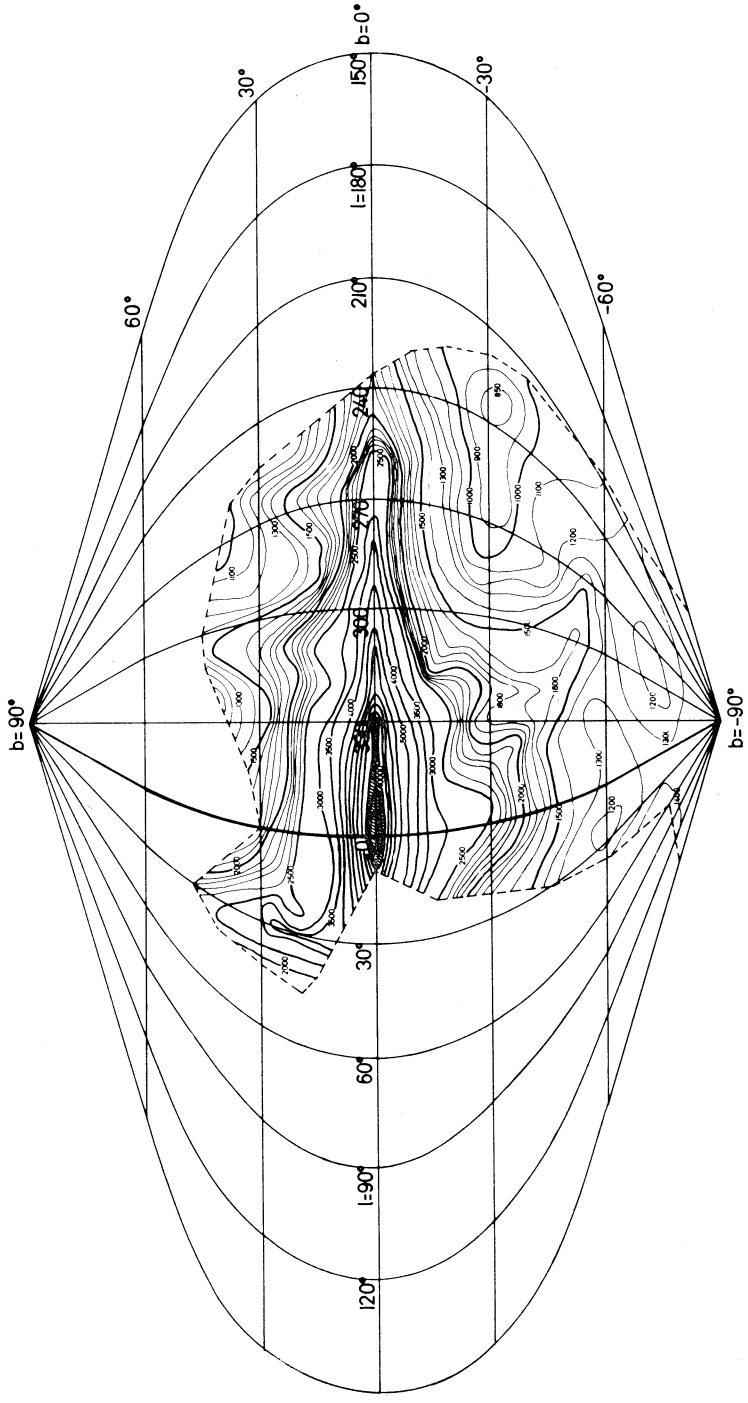


Fig. 5.—Galactic map showing modified beam temperatures with strong discrete sources removed.

mean over the entire forward response of the aerial, i.e. over the full-beam and sidelobe regions. The modified beam temperature  $T'_B$  is

$$T'_B = (\Omega_B + \Omega_S)^{-1} \int_{\Omega_B + \Omega_S} T(\theta, \phi) f(\theta, \phi) d\omega$$

and hence

$$\begin{aligned} T'_B &= \left( \frac{\Omega}{\Omega_B + \Omega_S} \right) T_i - \left( \frac{\Omega_G}{\Omega_B + \Omega_S} \right) T_G \\ &= 1.23 T_i - 0.24 T_G. \end{aligned}$$

We considered  $T_G$  independent of elevation and set it equal to 280°K (ambient temperature). Then

$$T'_B = 1.23 T_i - 70^\circ\text{K}.$$

## V. RESULTS

Contours of modified beam temperatures  $T'_B$  are plotted in equatorial coordinates in Figures 4(a)–4(c) and in galactic coordinates in Figure 5. To facilitate study of galactic features all sources included in the Mills, Slee, and Hill (1960, 1961) catalogues

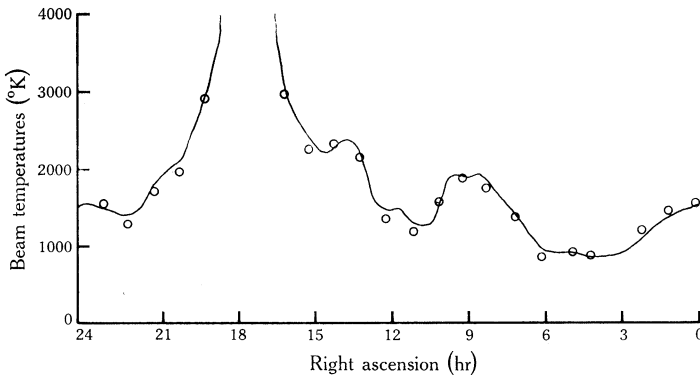


Fig. 6.—Comparison of modified beam temperatures (curves) with values of computed full-beam temperatures (○) for  $\delta = -33^\circ$  observed with the telescope pointing to the zenith.

that contributed more than 100°K to the aerial temperature were removed from the galactic map. Incomplete removal of extended sources such as Centaurus and Vela Puppis may have led to contour errors in these regions.

Two additional investigations were performed to enable estimation of errors in our sky map. In one investigation aerial temperatures were measured over a 24 hr period with the survey pointing to the zenith. In this experiment the ground contribution remained constant. The mean temperature in the sidelobe region was found from broad-beam absolute temperature measurements at the same frequency (Yates and Wielebinski 1966). In Figure 6 plots of  $T'_B$  from previous observations for  $\delta = -33^\circ$  (also observed at zenith) are compared with computed true full-beam temperatures. The maximum error observed in the temperature contours is  $\pm 100$  degK. To estimate the errors due to changes in ground contribution

with aerial elevation, cold sky areas were tracked from  $30^\circ$  above the horizon to the zenith. This experiment established that the maximum elevation correction for ground contribution is 5%. Because of the small and variable nature of this correction, modified beam temperatures were plotted and this error was incorporated in the overall survey error.

## VI. ERRORS

Our contour maps have two types of error. There is an error in the base temperature of the survey that is associated with systematic errors in the absolute temperature calibrations of the reference source and in the determination of the aerial parameters. There is also a relative error between any two directions. This error is associated with errors in determination of aerial parameters, observational errors including changes of ground and sidelobe contributions, and random mismatch errors. We have already discussed the errors associated with the imperfect reduction to modified beam temperatures. The value of this error is less than  $\pm 2\%$ . Absolute accuracy of the calibration source is estimated at  $\pm 1\%$ . Estimates of errors in the computation of spillover components are  $\pm 4\%$ . The ground contribution variation with elevation was found to be  $\pm 5\%$ . The random errors due to mismatch in the system were estimated at  $\pm 2\%$  from the scatter of observed south pole temperatures. An overall r.m.s. departure of the full-beam temperatures from the modified beam temperatures shown in the maps is therefore 7%.

## VII. DISCUSSION

The observations have been reduced to sky maps for galactic studies. The implications of the derived results on current galactic theories will be fully discussed in a later paper. In the present paper we confine ourselves to general remarks on the features and a comparison with the northern results.

Apart from the concentration of radiation along the galactic plane and towards the galactic centre, the most noticeable features are the spur-like feature extending from the plane to  $l^{\text{II}} = 320^\circ$ ,  $b^{\text{II}} = 45^\circ$  and the extended cold region centred on  $l^{\text{II}} = 250^\circ$ ,  $b^{\text{II}} = 35^\circ$ . For much of its length the spur feature lies on the same small circle that Quigley and Haslam (1965) fitted to both the northern spur and the feature north of the plane at  $l^{\text{II}} = 270^\circ$ . The cold region corresponds in position and temperature to the minimum observed in the northern galactic hemisphere.

Comparison of our survey with the survey of Baldwin (1955*a*) shows good agreement in the overlap regions. The temperatures are consistent after an allowance for the small frequency difference and greater beamwidth has been made. A maximum difference of 10% in the coldest temperature observed in the two surveys is possible within the error range.

It is intended to use the present results with those of the northern hemisphere to set up a galactic model. We are at present engaged in making scaled measurements at 408 MHz with the 45' reflector at Fleurs to provide spectrum results to further define the model.

## VIII. ACKNOWLEDGMENTS

The work described in this paper is a part of the research programme of the School of Electrical Engineering, University of Sydney. We wish to thank Dr. E. G. Bowen and Mr. J. Bolton, CSIRO, for permission to use the 210 ft telescope and the telescope operators at Parkes for assistance in making the observations.

Two of us (K.W.Y. and T.L.L.) have been supported by Commonwealth Scholarships.

## IX. REFERENCES

- BALDWIN, J. E. (1955a).—*Mon. Not. R. astr. Soc.* **115**, 684.  
BALDWIN, J. E. (1955b).—*Mon. Not. R. astr. Soc.* **115**, 690.  
BALDWIN, J. E. (1963).—*Observatory* **83**, 153.  
CHRISTIANSEN, W. N., and WELLINGTON, K. J. (1966).—*Nature, Lond.* **209**, 1173.  
CONWAY, R. G., KELLERMAN, K. I., and LONG, R. J. (1963).—*Mon. Not. R. astr. Soc.* **125**, 261.  
HARRIS I. A. (1961).—*Proc. Instn elect. Engrs B* **108**, 651.  
MILLS, B. Y. (1959).—*Publs astr. Soc. Pacif.* **71**, 267.  
MILLS, B. Y., HILL, E. R., and SLEE, O. B. (1958).—*Observatory* **78**, 116.  
MILLS, B. Y., SLEE, O. B., and HILL, E. R. (1960).—*Aust. J. Phys.* **13**, 676.  
MILLS, B. Y., SLEE, O. B., and HILL, E. R. (1961).—*Aust. J. Phys.* **14**, 497.  
MINNETT, H. C., and YABSLEY, D. E. V. (1966).—*Proc. Instn Radio Engrs Aust.* **27**, 304.  
PAULINY-TOTH, I. I. K., and SHAKESHAF, J. R. (1962).—*Mon. Not. R. astr. Soc.* **124**, 61.  
QUIGLEY, M. J. S., and HASLAM, C. G. I. (1965).—*Nature, Lond.* **208**, 741.  
SEEGER, CH. L., WESTERHOUT, G., CONWAY, R. G., and HOEKEMA, T. (1964).—*Bull. astr. Inst. Neth.* **18**, 11.  
TURTLE, A. J., and BALDWIN, J. E. (1962).—*Mon. Not. R. astr. Soc.* **124**, 459.  
YATES, K. W., and WIELEBINSKI, R. (1966).—*Aust. J. Phys.* **19**, 389.

